Paper presented at the ICMHR Conference, Darwin, Australia, July 2016

An Investigation into the Performance of Screw Feeders used in Bulk Solid Densification Processes

Alan W. Roberts, Timothy J. Donohue, Dusan Ilic, George Wakeman

TUNRA Bulk Solids Handling Research Associates, Newcastle Institute for Energy and Resources, The University of Newcastle, Australia

ABSTRACT The focus of this paper is on the design and performance of specialised screw feeders, which are employed to densify bulk solids as a means of meeting specific process plant requirements. Applications include de-aeration coupled with the achievement of higher packing densities and in other cases, dewatering of wet bulk solids including sludge and compost types of materials. Densifying screw feeders require careful consideration of the bulk density and associated packing ratios of the bulk solids in relation to the major consolidation stresses. The selection of suitable screw feeder geometries to achieve the desired densification along with the nominated feeder throughput requirements is outlined. The methodology for the determination of the screw axial loads, drive torques and power is also presented.

1. INTRODUCTION

Screw feeders are employed extensively in the bulk solids handling and process industries. Their versatility combined with innovative design allows them to be employed to meet the dual functions of controlled feeding at the required tonnage rates, as well as conditioning of the bulk solids to meet the necessary requirements of the process, such as the prevention of segregation and, in the case of fine powders, prevention of flooding and dust emission. The more common application is the mass-flow hopper and screw feeder combination where the screw functions as a variable capacity conveyor with the feed rate increasing from the rear of the hopper to the discharge end in such a manner to achieve, as near as possible, uniform draw-down of the bulk solid in the hopper without material compaction or blockages. A common arrangement is to employ a screw geometry incorporating a converging tapered shaft in combination with an expanding screw pitch.

The specific focus of this paper is on another group of specialised screw feeders employed for densifying bulk solids. Such applications include the need to compress loosely packed bulk solids to achieve higher packing densities coupled with de-aeration to expel entrained air, and in some cases, to achieve high consolidating pressures for pelletising operations. Another area involves the application of screw presses for dewatering processes for saturated sludge and compost types of materials. As illustrated by Figure 1, a typical geometrical form of densifying screw feeder comprises a combination of diverging tapered shaft and contracting screw pitch. This is completely the opposite of the conventional screw feeder and mass-flow hopper combination.

The purpose of this paper is to provide a detailed review of the design objectives of densifying screw feeders. The measured flow properties of the bulk solids, particularly the interrelation of the bulk and packing densities with the major consolidation stresses is shown to have a major influence on the selection of the most appropriate screw geometry and the determination of the axial loads, drive torques and powers. The paper presents a theoretical analysis of the performance of densifying screws aimed at the selection of the optimal screw geometrical combinations for a diverging tapered shaft and contracting screw pitch in the conveying or feeding direction. The influence of an extruded plug arrangement with back pressure control at the discharge end of the screw feeder is also examined. The paper draws upon background research into screw conveyor and feeder performance as illustrated in previous work [1-5].

2. DENSIFYING SCREW FEEDERS

The general form of a densifying screw feeder is shown in Figure 1, in which the progressive consolidation of the bulk solid through the screw is achieved by a combination of diminishing screw pitch and diverging shaft taper in the direction of feed. The performance objectives of such feeders are to achieve the required level of compaction, without the occurrence of jamming of the bulk solid within the screw, a somewhat stringent design target. For de-aeration applications, the casing of the feeder needs to be appropriately vented to permit the expulsion of the released air. For dewatering screw presses, the casing is also designed as a screen to allow the released water to be progressively drained away.

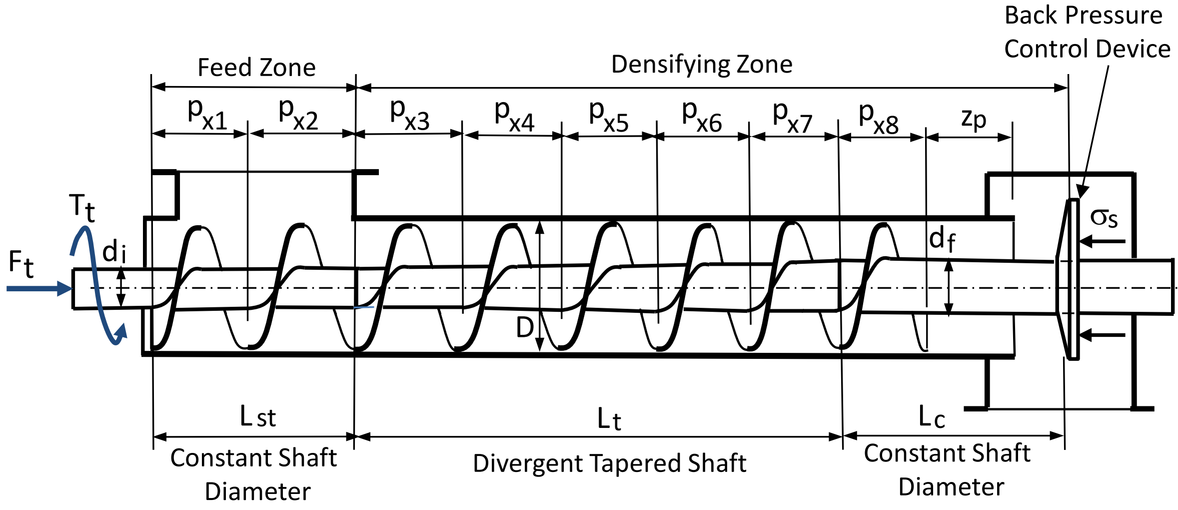

Figure 1 Densifying Screw Feeder

2.1 Performance and Design Objectives

Apart from a complete set of relevant flow properties necessary for the design of the screw, it is particularly important to consider carefully the bulk and packing densities as functions of the major consolidation stress. This is depicted in Figure 2. As a typical example, this set of graphs, applies to a particular by-pass coal at 16% moisture content.

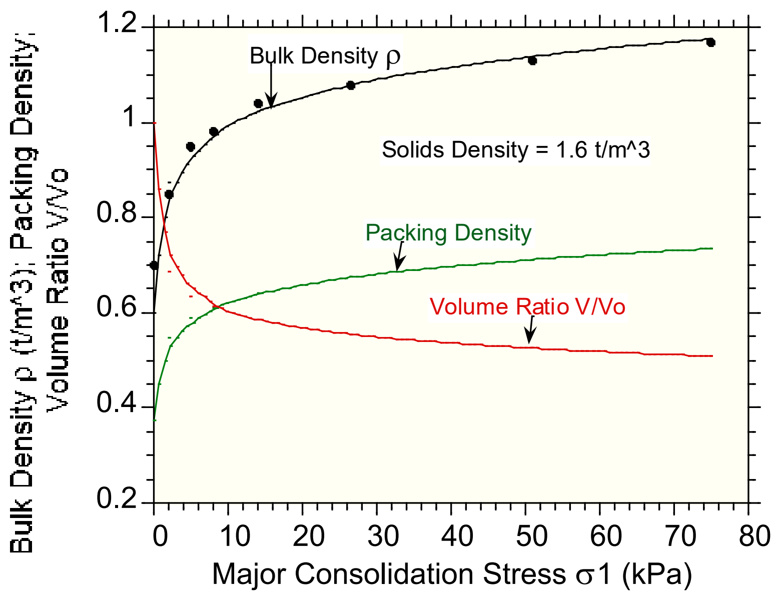

Figure 2 Bulk Density, Packing Density and Volume Ratio By-Pass Coal at 16% Moisture Content

Flow property tests performed on bulk solids show that the bulk density ρ versus major consolidation stress σ_1, can be represented by the following relationship:

$$\rho = C_1 \sigma_1^{C_2} \quad (1)$$

For the By-Pass Coal, the measured data can be represented by equation (1) with the assigned values $C_1 = 0.825$ and $C_2 = 0.082$. For screw design, it is usually the case that the bulk density is known, requiring the corresponding major consolidation stress to be determined. Hence, equation (1) becomes

$$\sigma_1 = \left(\frac{\rho}{C_1}\right)^{\frac{1}{C_2}} \quad (2)$$

Based on the solids density of the coal, $\rho_s = 1.6\ t/m^3$, the packing density $= \frac{\rho}{\rho_s}$ is also plotted in Figure 2. The selection of screw geometry is dependent on the need to progressively decrease the screw pitch volume, thus increasing the bulk density and packing ratio in the direction of feed. To this end, the pitch volume V as a ratio of the volume V_o at the feed or intake point is also plotted in Figure 2. The volume ratio is given by

$$\frac{V}{V_o} = \frac{\rho_o}{\rho} \quad (3)$$

where V_o = screw pitch volume at feed point
ρ_o = bulk density at feed point

It is quite apparent from Figure 2 that the rate of consolidation relative to the consolidation stress σ_1 is greatest at the feed end of the conveyor where the initial bulk density and consolidation stresses are quite low. However, as the consolidation continues along the screw, small decreases in screw space volumes are accompanied by substantial increases in consolidation stresses requiring high drive torques with the possibility of particle degradation due to attrition. By way of example, for the By-Pass Coal of Figure 2, it would seem reasonable to limit the densification corresponding the consolidation stress, say σ_1 = 60kPa. Where additional densification is required, this may be achieved via the application of the extruded plug depicted in Figure 1.

3. MECHANICS OF CONVEYING ACTION

The basic mechanics of screw conveyor operation, as previously presented in [1-5] is now reviewed. Figure 3 shows a section of a screw conveyor inclined at an arbitrary angle of θ and operating at a particular rotational speed, ω. Consider a single particle in contact with the screw surface at a nominated radius "r" as shown. The velocity diagram for the particle is shown in Figure 3 and reproduced in Figure 4.

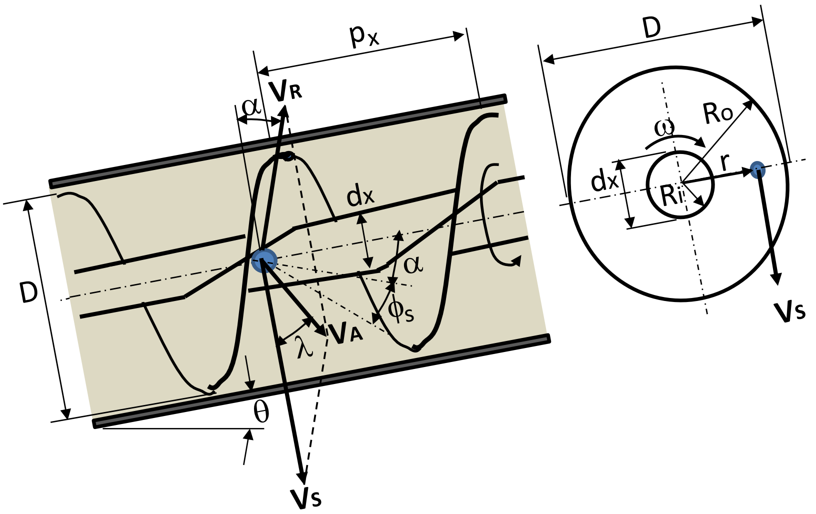

Figure 3 Mechanics of Screw Conveying

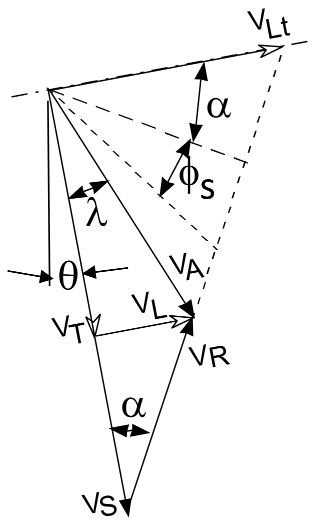

Figure 4 Velocity Diagram

3.1 Particle Velocities

The velocity components are:

V_S = screw velocity; V_R = relative velocity; V_A = vector sum of V_S and V_R = absolute velocity

The screw velocity is given by

$$V_S = r\,\omega \quad \text{(m/s)} \tag{4}$$

where $\omega = \frac{\pi N}{30}$ angular velocity N = rotational speed rev/min

V_A is the absolute velocity of the particle which moves in a helical path, defined by the helix angle λ, of opposite hand to that of the screw. The absolute velocity V_A has two components, the axial conveying component V_L and the rotational or vortex component V_T. Since the helix angle α of the screw flight varies with the radius, being smaller at the outer periphery and larger at the shaft, the angle λ will also vary in the radial direction from the outside of the flight to the shaft. Hence the conveying action is more efficient at the region of the outer radius of the helical flight than in the central region adjacent to the shaft. The variation in V_T with radius describes the vortex motion in the screw which is given by the general relationship

$$V_T\, r^n = C \tag{5}$$

where r = radius C = constant n = vortex index

Previous research [1, 3] has shown that the operation of a screw conveyor at a particular rotational speed is such that the vortex index $n \approx 0$ for which $V_T \approx$ constant.

The velocity V_{Lt} shown in Figure 4 is the maximum theoretical velocity for the idealised case of the screw operating 100% full and the bulk solid moving axially without rotation. This cannot be achieved in practice since the axial conveying velocity V_L is a function of the path helix angle λ which depends on the screw geometry, friction angle for the bulk solid in contact with the screw flight, angle of elevation, and conveyor speed. In general, the angle λ is

$$\lambda \leq [90^o - (\alpha + \phi_s)] \tag{6}$$

ϕ_s = friction angle for bulk material on screw flight

3.2 Conveyor Throughput and Volumetric Efficiency

For design purposes, it has been shown to be acceptable to lump the bulk solid rotational mass for each pitch at the effective screw radius defined by

$$R_e = \frac{2}{3}\left[\frac{R_o^3 - R_i^3}{R_o^2 - R_i^2}\right] = \text{effective radius of screw} \tag{7}$$

$R_o = \frac{D}{2}$ = outer screw radius $R_i = \frac{d}{2}$ = inner screw radius

The corresponding effective helix angle α_e is

$$\alpha_e = \tan^{-1}\left[\frac{p_x}{2\,\pi\,R_e}\right] \tag{8}$$

The volumetric throughput in m^3/rev for each pitch of the screw conveyor is given by

$$Q = Q_t\,\eta_V \quad (m^3/\text{rev}) \tag{9}$$

where Q_t = maximum, idealised throughput defined by

$$Q_t = \pi (R_o^2 - R_i^2)(p_x - t_s) \quad (m^3/rev) \tag{10}$$

η_V = volumetric efficiency p_x = screw pitch t_s = screw blade thickness

The corresponding mass feed rate is

$$Q_m = \rho Q \quad (t/rev) \tag{11}$$

where ρ = bulk density (t/m^3) for the specific screw pitch space

In the case of the conveyor running 100% full, the volumetric efficiency is given by

$$\eta_V = \frac{V_{Le}}{V_{Lt}} = \frac{\tan \lambda e}{\tan \alpha_e + \tan \lambda e} \tag{12}$$

(a) General Case: Operation at Arbitrary Elevation Angle

The application of equation (12) requires a knowledge of the relevant path helix angle λ_e which depends on the screw geometry, rotational speed, angle of elevation and the properties of the bulk solid being conveyed. In the absence of more a detailed analysis, the following empirical equation may be used to predict the effective path helix angle λ_e .

$$\lambda_e = \lambda_{e\_max} \left(1 - \frac{\sin \theta}{3}\right) \tag{13}$$

where θ = angle of inclination of the screw conveyor

The angle λ_{e_max} is the maximum value of λ_e based on a particle in contact with the helical blade of the screw. It is defined by

$$\lambda_{e\_max} = [90^o - (\alpha_e + \phi_s)] \tag{14}$$

The angle λ_{e_max} is substituted in equation (12) to compute the volumetric efficiency of the screw conveyor.

(b) Special Case of Horizontal Screw Feeder Conveyor

In this case, it may be assumed that the motion of the bulk solid through the conveyor corresponds to the maximum value λ_{emax} defined by equation (13). With this value substituted in equation (12), it can be shown that the volumetric efficiency of a horizontal screw conveyor is given by

$$\eta_{Vmax} = \frac{1}{\tan \alpha_e \tan(\phi_s + \alpha_e) + 1} \tag{15}$$

4. AXIAL FORCES DUE TO CONVEYING ACTION

The forces acting on the screw blade of the densifying screw are now considered:

4.1 Force F_{A1} to Compress Bulk Solid

The force $F_{A1} = \frac{\pi}{4}(D^2 - d^2)\,\sigma_1$ is applied to continually compress the bulk solid, expel contained air and/or moisture and to increase the packing density as the solid is transported axially through the conveyor. The compression process is accomplished by the decreasing screw space volume along the screw. Under the action of the force F_{A1}, the compression of the bulk solids in each pitch space, p_x, occurs between the front driving face of the helical screw blade and the trailing face of the leading pitch. Hence the torque contribution due to "double shear" on the helical blade surfaces needs to be included in the calculations.

4.2 Force F_{A2} to Convey the Bulk Solid due to Consolidation Stress σ_1

The consolidation stresses σ_1 give rise to the normal stresses $\sigma_{n1} = k\ \sigma_1$ acting radially outward against the casing as illustrated in Figure 5. Because the screw rotates at very low speeds, the normal stress component due to centrifugal effects are negligible. It is assumed that an active state stress exists within the screw pitch space, for which the stress ratio k<1. The value k =0.6 has been assumed in the example presented in Section 8.

$$F_{A2} = \mu_c\, p_x\, \pi\, D\ \sigma_{n1} \qquad (16)$$

where $\mu_c = \tan \phi_c$ = friction coefficient for axial motion of the bulk solid in contact with the casing. ϕ_c = corresponding casing friction angle.

4.3 Force F_{A3} to Convey the Bulk Solid due to Weight of Bulk Solid

The normal stress σ_{n2} of Figure 5 arises as a result of the weight of bulk solid in the screw pitch space. It is assumed that the screw operates 100% full. The stress σ_{n2} is not constant but varies around the screw as depicted in Figure 5. It is zero at the top of the casing and a maximum at the bottom:

$$\sigma_{n2\_max} = \gamma\, D \cos\theta \qquad (17)$$

From a study of the stress field, it may be shown that the axial force to convey the bulk solid along the casing is given by

$$F_{A3} = \gamma\, \pi\, p\, \frac{(D^2 - d^2)}{4}\, (\sin\theta + \mu_e \cos\theta) \qquad (18)$$

where $$\mu_e = \frac{2\,\mu_c}{1 + \sin\delta} \qquad (19)$$

$\gamma = \rho\, g$ = bulk specific weight $\qquad \mu_c$ = casing friction coefficient

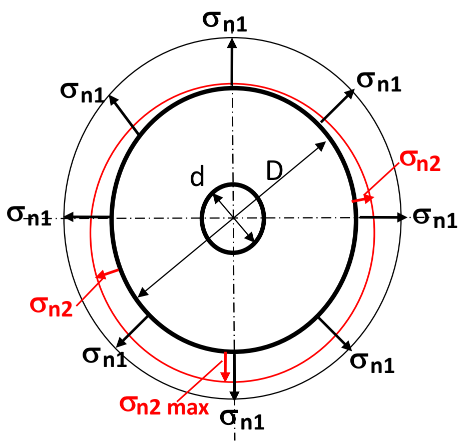

Figure 5 Normal Stresses Acting Around Casing

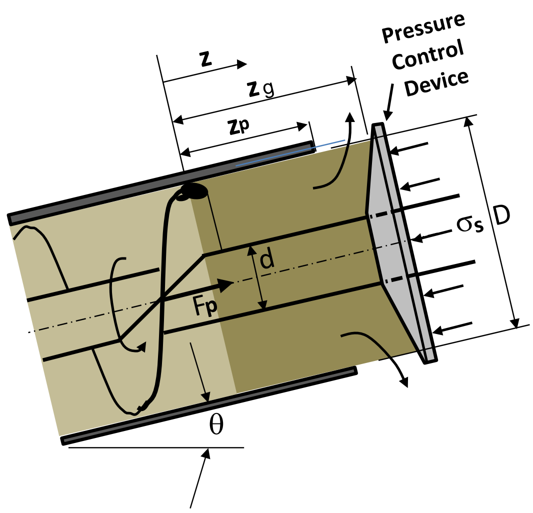

Figure 6 Forces Acting on Plug

5 FORCES TO EXTRUDE AND CONVEY PLUG AGAINST APPLIED BACK PRESSURE

The forces acting on the plug at the discharge end are depicted in Figure 6. Two axial force components are considered, the force to compress the bulk solid in the plug and the force to convey the plug.

5.1 Force F_{P1} to compress the Bulk Solid

The axial pressure exerted by the screw at the coordinate position z is given by

$$\sigma_z = K\, e^{C_3 z} - \frac{\gamma_z}{C_3} \tag{20}$$

where $c_3 = 4\,k\left(\frac{\mu_c D - \mu_s d}{D^2 - d^2}\right)$ (21) and $K = \left(\sigma_s + \frac{\gamma_z}{C_3}\right) e^{-C_3 z_g}$ (21)

The force to extrude the plug is given by equation (20) at z = 0. That is

$$F_{p1} = \frac{\pi}{4}\,(D^2 - d^2)\left(K - \frac{\gamma_z}{C_3}\right) \tag{22}$$

5.2 Plug Conveying Forces

There are additional axial forces, $\mathbf{F_{p2}}$ and $\mathbf{F_{p3}}$ due to the conveying of the plug along the casing at the exit end of the screw.

(a) Force to Convey Plug Under Action of Normal Stress due to Axial Compression

$$F_{p2} = \mu_c\, k_a\, \sigma_1\, \pi\, D\, p_x \tag{23}$$

(b) Force to Convey Plug Under Action of Plug Weight

$$F_{p3} = \gamma_z\, \pi\, p_x\, \frac{(D^2 - d^2)}{4}\,(\sin\theta + \mu_e \cos\theta) \tag{24}$$

where μ_e is defined by equation (19). $k_a = 0.6$ is chosen for the present study

6. SUMMARY – TOTAL AXIAL FORCE ACTING ON SCREW THRUST BEARING

The force acting on the screw shaft thrust bearing is the sum of the conveying forces per pitch plus the axial forces generated by the plug. It excludes the double acting force components F_{A1}.

$$F_{At} = \sum_1^m (F_{A1} + F_{A2} + F_{A3}) + F_{p1} + F_{p2} + F_{p3} \tag{25}$$

where m = number of pitch lengths along screw

7. TORQUE AND POWER FOR DENSIFYING SCREW CONVEYOR

Each of the foregoing axial force components is converted into corresponding drive torque components taking into account the relevant bulk solid and screw surface friction angles and effective screw helix angle. For each pitch length of the screw, the following general equation for the torque calculations applies.

$$T = F_A\, R_e \tan(\alpha_e + \phi_S)\, K_S \quad \text{(kNm)} \tag{26}$$

Where R_e = effective screw radius α_e = effective helix angle ϕ_s = screw surface friction angle

The parameter K_S takes into account the frictional drag due to the pressure on the rear surface of the leading pitch. For the compressive component due to F_{A1}, K_S is selected in the range 1.5 to 2.0. For all other components it has been assumed that K_S = 1.0 to 1.2.

In addition to the above, the drive torque component to overcome the shaft frictional resistance needs to be determined.

$$T_{sh} = \mu_{sh}\ \sigma_{n1}\ \pi \frac{d^2}{2}\ p_x \qquad \text{(kNm)} \tag{27}$$

where μ_{sh} = coefficient of friction for shaft
σ_{n1} = normal stress as defined in Section 4.2

7.1 Total Torque

The total torque T_t required to convey the bulk solid is the summation of the torque components T_i over the length of the screw. That is $T_t = \sum_m T_i$, where m = number of pitches along the screw

7.2 Drive Power

$$\text{Power} = \frac{0.105 N\, T_t}{\eta_d} \tag{28}$$

where N = rpm η_d = drive efficiency

8. DESIGN EXAMPLE

The following example based on the screw geometry of Figure 1 handling the By-Pass Coal with properties exhibited in Figure 2 at a throughput of 20t/h is presented. The screw feeder is operating at an inclination angle of 20°. The bulk density at the loading or intake end of the screw feeder is 0.65t/m^3. Table 1 lists the design input data for the feeder and for the plug at the discharge end. Based on the bulk density data plotted in Figure 2, the backpressure control is set at 24kPa. The relevant screw geometry data is tabulated in Table 2. The screw diameter D is 0.45m. To assist in smoothing the screw intake, the screw pitch has progressive incremental increases from 0.425m to 0.45m in the feed zone. In the densifying zone, the pitch decreases in steps to 0.325m remaining at this value for the last screw pitch and plug zone. The shaft diameter is 0.15m in the feed zone, the diameter then increasing via a diverging taper to 0.22m over the length of L_t = 1.47m, then remaining constant at 0.22m. Table 3 summarises the final performance data obtained from the design analysis.

8.1 Computed Results

Figure 7 shows the variations in bulk density ρ, consolidation stress σ_1 and volumetric efficiency η_V along the screw. Over the first conveying section, the densification increases at quite a low rate, but then increases significantly almost immediately following the intake section. The rapid increase in consolidation stress beyond x = 2m is very significant. It is also interesting to note that the volumetric efficiency, and hence conveying efficiency, increases along the screw. This is quite the opposite of the traditional hopper and screw feeder.

For axial conveying, it is necessary to ensure that the casing is able to provide sufficient restraining torque resistance to offset the torque generated by the rotating helical screw flight. The following "Ratio" is a useful measure of the condition governing axial conveying:

$$\text{Ratio} = \frac{\text{Screw Torque per pitch}}{\text{Casing Restraining Torque } T_{res}} \tag{29}$$

where $$T_{res} = \mu_{cr}\, p_x\, \pi \left(\frac{D^2}{2}\, \sigma_{n1} + \rho\, g\, \frac{(D^2 - d^2)}{4} \cos\theta \right) \tag{30}$$

μ_{cr} = casing friction coefficient in the circumferential direction. Other variables as previously defined.

For the particular example being considered, Figure 8 shows the torque ratio increasing along the screw, the ratio approaching the conveying limit at the exit end. For the condition Ratio < 1.0 the circumferential friction is not fully mobilised, ensuring efficient axial conveying. For Ratio ≥ 1.0, the casing friction is fully mobilised leading to less efficient axial conveying with the possibility for jamming to occur.

TABLE 1 - SCREW FEEDER DESIGN DATA

SCREW DESIGN DATA		
Throughput (m^3/h)	Q_m	20.00
Inclination Angle (deg)	θ	20.00
Screw Diameter (m)	D_o	0.45
Tapered Shaft Initial Diameter (m)	d_i	0.15
Tapered Shaft Final Diamater (m)	d_f	0.22
Length of Taper (m)	L	1.470
Length to Start of Taper (m)	L_{st}	0.875
Av. Blade thickness (m)	t_s	0.02
Screw & Shaft Friction Angle (deg)	ϕ_s	20.00
Casing Friction Angle (deg)	ϕ_c	30.00
Bulk Density at Feed End (t/m^3)	ρ_i	0.65
Effective Internal Friction Angle (deg)	δ	50.00
Drive Efficiency	η_d	0.85
PLUG DESIGN DATA		
Plug Length (m)	z_p	0.33
Plug Diameter (m)	D_{pg}	0.45
Plug Inner Diameter (m^2)	d_p	0.22
Plug Area (m^2)	A_p	0.12
Plug Casing Length (m)	z_c	0.22
Bulk Density in Plug Zone (t/m^3)	ρ_p	1.09
Gate Control Pressure (kPa)	σ_s	24.00

TABLE 2 - SCREW GEOMETRY

Pitch	x (m)	p_x (m)	d_x (m)	α_e (deg)
1	0.425	0.425	0.150	22.60
2	0.875	0.45	0.150	23.78
3	1.285	0.41	0.170	21.70
4	1.655	0.37	0.187	19.44
5	2.005	0.35	0.204	18.17
6	2.345	0.34	0.220	17.41
7	2.675	0.33	0.220	16.79
8	3	0.325	0.220	16.55
Plug 9	3.45	0.325	0.220	16.55

TABLE 3 - SUMMARY OF RESULTS

Throughput (m^3/h)	Q_m	20.00
Screw Speed (rev/min)	N	11.50
Screw Speed (rad/sec)	ω	1.20
Axial Force (kN)	F_A	17.30
Torque to Compress Coal (kNm)	T_s	2.62
Torque to Convey Coal (kNm)	T_c	2.59
Torque due to Shaft (kNm)	T_{sh}	0.45
Total Torque (kNm)	T	5.66
Power (kW)	P_s	8.02

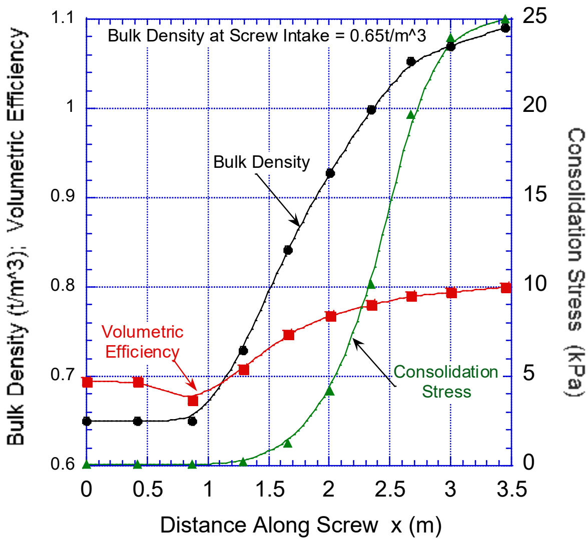

Figure 7 Densifying Screw Feeder Performance

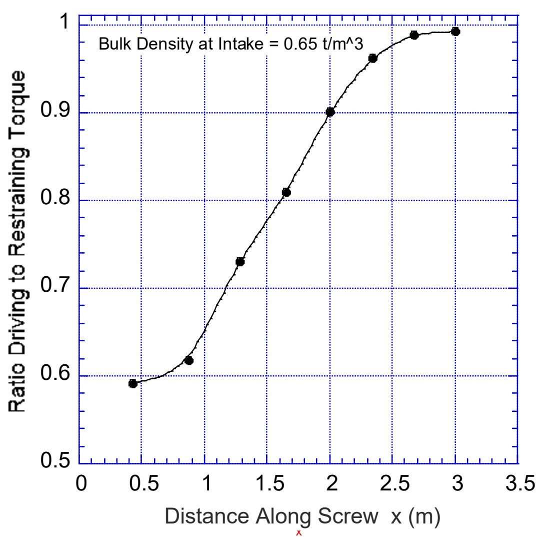

Figure 8 Ratio of Screw Driving Torque to Casing Restraining Torque

8.2 Effect of Variation in Bulk Density at Intake

The bulk density of the bulk solid entering the densifying screw feeder at the feed point has a significant influence of the feeder performance. For the example under consideration, this is demonstrated by the results plotted in Figures 9, 10 and 11 which examine the influence of changes in the initial bulk density at the screw intake from 0.6t/m^3 to 0.8t/m^3. In each Figure, two sets of results are presented: one set shown by full lines applies to the screw feeder with divergent tapered shaft of the design example under consideration. The second set, shown by dotted lines, applies to an alternate feeder with a parallel constant diameter shaft.

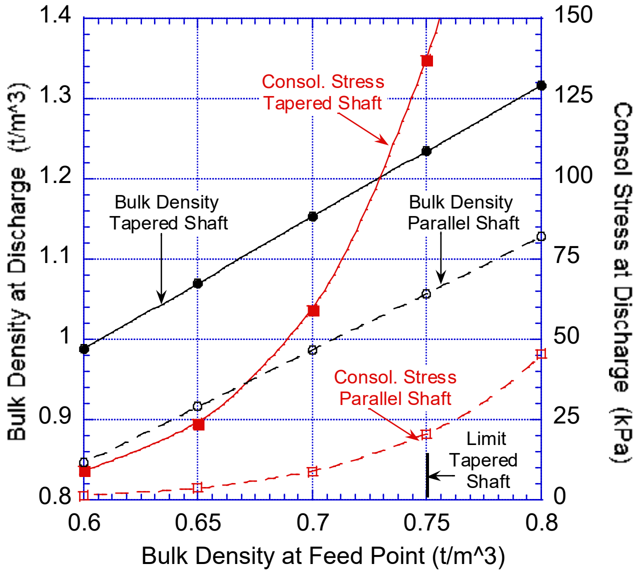

Figure 9 Bulk Density and Consolidation Stress at Discharge Versus Initial Bulk Density

As shown by Figure 9, the bulk density at discharge increases linearly with the increase in the bulk density of the screw feed, but the corresponding increase in consolidation stress at the discharge end of the screw is highly nonlinear and more significant for the tapered shaft. This would suggest that for the chosen screw geometry of Table 2, the intake bulk density should be limited to the maximum value of 0.75t/m^3. This limit is imposed on the full line performance results of Axial Force, Torque, Power and screw speed plotted in Figures 10 and 11.

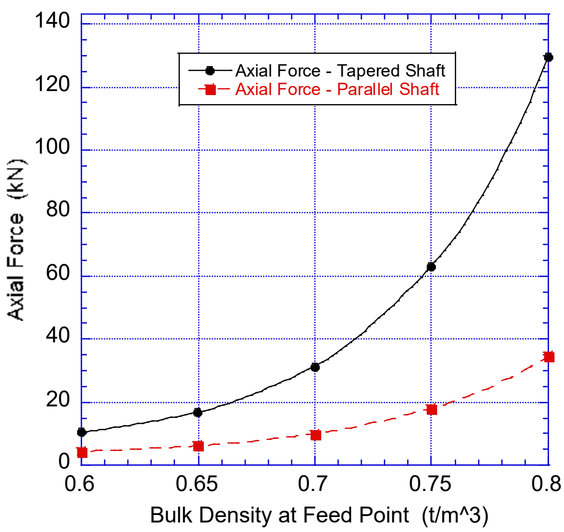

Figure 10 Axial Force Versus Initial Bulk Density

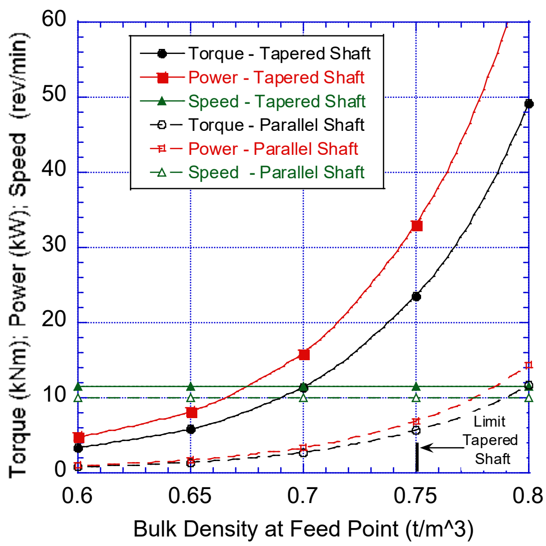

Figure 11 Torque, Power and Speed Versus Initial Bulk Density

9. CONCLUDING REMARKS

The versatility of screw feeding equipment for bulk solids processing operations has been demonstrated in this paper, in which the focus is specifically on the design and performance of screw feeder conveyors employed to densify bulk solids. The design of such screw feeding equipment is highly dependent on the flow properties of the bulk solid, notably the bulk density versus consolidation stress characteristics and packing ratios, and the manner in which these properties influence the selection of the most appropriate screw geometry.

The paper has demonstrated the important interrelation between the bulk density of the bulk solid at the intake, or feed point, with that of the required level of densification at the feeder discharge. The basic approach and methodology for the design of screw conveyors and feeders has been reviewed and modified to meet the specific design approach necessary for the design of densifying screw feeding equipment.

The material presented in the paper covers the initial stage of an ongoing study into the performance of densifying screw feeders. Follow up research includes Discrete Element Modelling (DEM) simulation coupled with experimental studies.

10. REFERENCES

[1] Roberts, A.W. An Investigation of Grain Vortex Motion with Relation to the Performance within Vertical Grain Augers". Proc. of the Instn. of Mech. Engrs, 178 (1963-1964), 293.

[2] Roberts, A.W. Predicting the Volumetric and Torque Characteristics of Screw Feeders. Bulk Solids Handling, Vol. 16, No 2, 1996, (pp.233-244

[3] Roberts, A.W. The Influence of Granular Vortex Motion on the Volumetric Performance of Enclosed Screw Conveyors". Powder Technology, 104, (1999) 56-67.

[4] Roberts A.W. Design and Performance Criteria for Screw Conveyors in Bulk Solids Operation. Bulk Solids Handling, Vol 22, 2002, (pp.436-444)

[5] Roberts, A.W. Bulk Solids: Optimizing Screw Conveyors. www.Chemengonline.Com February 2015, (pp.62-68)